Pressure effects on the magnetoelectric properties of a multiferroic triangular-lattice antiferromagnet CuCrO₂

Takuya Aoyama,[1] Atsushi Miyake,[2] Tomoko Kagayama,[2] Katsuya Shimizu,[2] and Tsuyoshi Kimura[1]

[1]*Division of Material Physics, Graduate School of Engineering Science, Osaka University, Toyonaka, Osaka 560-8531, Japan*

[2]*KYOKUGEN, Research Center for Materials Science at Extreme Conditions, Osaka University, Toyonaka, Osaka 560-8531, Japan*

Effects of high pressure exceeding 10 GPa on spin-driven ferroelectricity were investigated for a multiferroic, triangular-lattice antiferromagnet (TLA), CuCrO₂. For this purpose, we developed a system which enables us to measure ferroelectric polarization under a pressure of 10 GPa by using a diamond anvil cell. We found that the magnetic transition temperature accompanying the ferroelectric one in CuCrO₂ was remarkably enhanced by applying pressure. The result is simply explained by considering the pressure-induced enhancement of inter- and/or intralayer magnetic interaction due to the compression of the lattice. In addition, the coercive electric field for the polarization reversal was also increased with increasing pressure, while the amplitude of the ferroelectric polarization was steeply suppressed at around 8 GPa. A possible origin of the observed pressure effects on the ferroelectric property in the multiferroic TLA is discussed in terms of a ferroelectric-antiferroelectric transition and structural domain rearrangement by uniaxial stress.

I. INTRODUCTION

Recently, it was found that CuCrO₂ with a delafossite structure exhibits ferroelectricity below $T_N = 24$ K (Refs. [1] and [2]), at which a magnetic order into a proper-screw-type spiral structure change takes place [Figs. 1(a)–1(d)].[3–5] In the delafossite structure (space group $R\bar{3}m$), Cr^{3+} ions ($S = 3/2$) form triangular-lattice planes (TLPs) stacked along the hexagonal c axis. On the TLPs, spin frustration arises, and then the screw spiral magnetic structure having the degree of freedom of spin chirality is stabilized to release the spin frustration. The ferroelectricity accompanied by the screw spiral order in CuCrO₂ is reasonably explained by the so-called "p-d hybridization model," in which electric polarization induced by a spin-dependent orbital hybridization between $3d$ (metal) and $2p$ (ligand) does not cancel out in a crystal when the crystal possesses relatively lower crystal symmetry.[6] According to a measurement of polarized neutron scattering on CuCrO₂, the reversal of the electric polarization by applying an electric field causes a reversal of the spin chirality.[5]

When Cu^{1+} ions in CuCrO₂ are replaced with smaller monovalent ions such as Li^{1+} and Na^{1+}, the delafossite structure [left illustration of Fig. 1(e)] transforms into the so-called ordered rocksalt structure in which the stacking pattern of the TLPs along the c axis is slightly different from that in the delafossite [right illustration of Fig. 1(e)].[7] Note that the c axis length as well as the inter-TLP distance of LiCrO₂ are much smaller than those of CuCrO₂, as illustrated in Fig. 1(e). Magnetic susceptibility, dielectric constant, and electric polarization in a single crystal of LiCrO₂ are also shown in Fig. 1.[8] Though the dielectric constant showed a small anomaly accompanied by a magnetic transition into a proper-screw magnetic-ordered state, finite electric polarization was not observed,[1] which is in sharp contrast with the case of delaffosite CuCrO₂. According to a former neutron scattering measurement on LiCrO₂, the spin chirality has an antiparallel arrangement between adjacent TLPs.[9] This configuration may cancel out the macroscopic polarization (i.e., antiferroelectric state), which is consistent with the absence of spin-driven ferroelectricity in LiCrO₂.[1] However, the origin of the alternating stacking of the spin chiral ordered state is still under debate.

In this paper, we report on effects of pressure on crystallographic structure, magnetism, and spin-driven ferroelectricity in the delafossite CuCrO₂. We discuss the relationship between the crystallographic structure and the spin-driven ferroelectricity in CuCrO₂ through continuous tuning of lattice parameters by means of applying external pressure. For this purpose, we developed a system which enables us to measure ferroelectric polarization under high pressure above 10 GPa by using a diamond anvil cell (DAC). As far as we know, no measurement of ferroelectric polarization has been reported under such high-pressure conditions. (There are several letters which report measurements of dielectric constant.[10,11]) Our system has sensitivity high enough to measure spin-driven ferroelectric polarization, which is generally $10^2 \sim 10^3$ times smaller than ferroelectric polarization in conventional ferroelectric compounds.

II. EXPERIMENTAL

Single crystals of CuCrO₂ were grown by the flux method as has been reported previously.[2] To study the pressure effect on the lattice, some of the crystals were crushed into fine powders, and powder x-ray diffraction (XRD) measurements were performed at room temperature under various pressures up to about 11 GPa by using a DAC with an 800-μm culet diameter diamond anvil. A mixture of methanol and ethanol with a 4:1 volume ratio was used as a pressure-transmitting medium. The x-ray wavelength was 0.7107 Å (Mo $K\alpha$), and an imaging plate (IP) was used as a detector of the diffracted x ray. For the image data processing and the refinement of lattice parameters an IP Analyzer was used.[12] To measure ac heat capacity C_{ac}, dielectric constant ε', and electric polarization P at high pressure, a crystal of CuCrO₂ with the dimensions of $\approx 100 \times 100 \times 20\,\mu m^3$ and the widest face normal to the [110] direction was loaded in a DAC with an anvil culet diameter
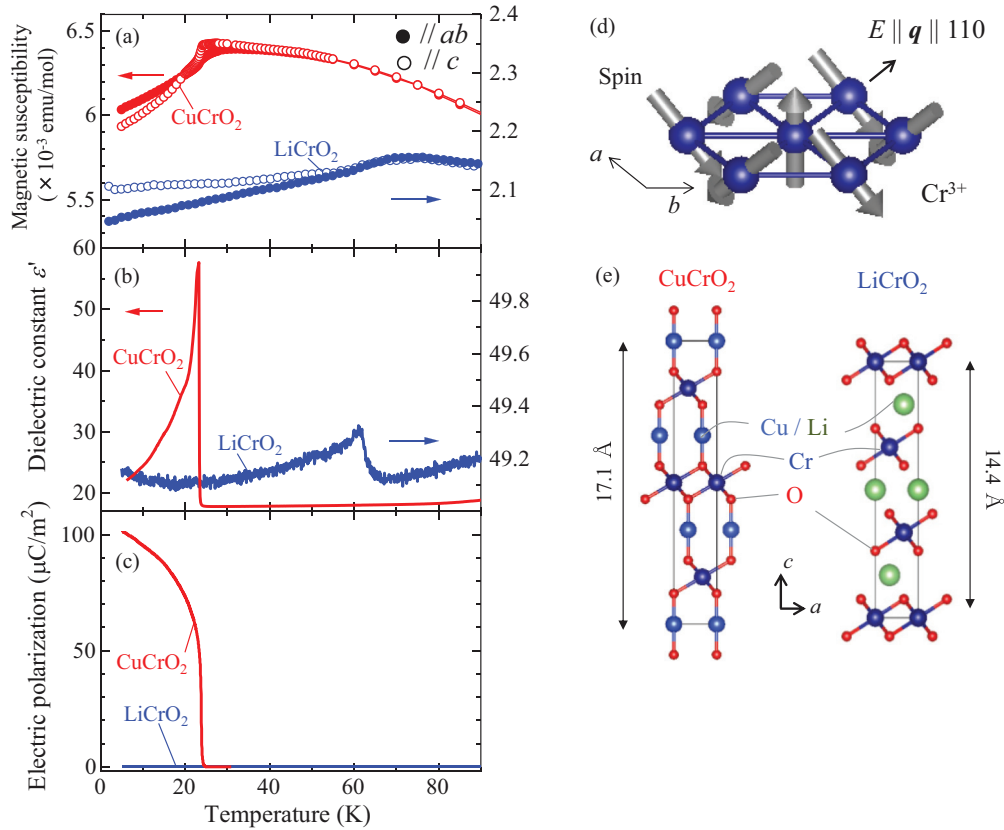
FIG. 1. (Color online) Temperature profiles of (a) magnetic susceptibility, (b) dielectric constant along the [110] direction, and (c) electric polarization along [110] for single crystals of CuCrO$_2$ and LiCrO$_2$. Closed (open) circles in (a) denote magnetic susceptibility perpendicular (parallel) to the c axis in the hexagonal setting. (d) Magnetic structure within the ab plane below T_N. (e) Crystal structures of CuCrO$_2$ (left) and LiCrO$_2$ (right).

of 600 μm. Then, the temperature (T) profiles of C_{ac}, ε', and P were measured at selected pressures by using a lock-in amplifier, an LCR meter, and an electrometer, respectively. A microscope image of the sample assembly in the pressure chamber through the diamond anvil for these measurements is shown in the inset of Fig. 3(a). Details of the experimental techniques have been reported in Refs. 11 and 13. Glycerin was used as a pressure-transmitting medium for the measurements of C_{ac}, ε', and P. The direction of an applied electric field E was along the [110] direction for both the ε' and P measurements. Before and after the respective measurements, applied pressure was determined by a ruby uorescence method at room temperature and 10 K. The differences of pressures between before and after the measurements are within 0.5 GPa.

III. RESULTS

To examine variations of lattice parameters and the presence (or absence) of a pressure-induced structural phase transition into the ordered rocksalt structure, we performed the powder XRD measurements at various pressures. The measurements were performed at room temperature upon the pressurizing process. Figure 2(a) shows XRD profiles at selected pressures. It is apparent that no significant change in the profiles was observed up to 11.3 GPa, suggesting that there is no structural phase transition in the pressure range studied here. Figure 2(b)

shows pressure variations of scaled lattice parameters, the a- and c-axis lengths (hexagonal setting). From these data, the isothermal compressibility $\kappa = -\frac{1}{V}(\frac{\partial V}{\partial p})_T$ along the a and c axes are estimated as $\kappa_a = (2.30 \pm 0.057) \times 10^{-3}$ GPa^{-1} and $\kappa_c = (3.92 \pm 0.866) \times 10^{-4}$ GPa^{-1}, respectively. Namely, notable anisotropic behavior was observed in κ of CuCrO$_2$. A similar anisotropic behavior has been reported for other delafossite families such as CuFeO$_2$ (Ref. 14) and CuGaO$_2$ (Ref. 15). The bulk modulus B and its pressure derivative B' were obtained from fitting volume variations by Murnaghan's equation, i.e., $p(V) = \frac{B}{B'}[(\frac{V_0}{V})^{B'} - 1]$, as shown in Fig. 2(c). Here, V_0 is the unit-cell volume under ambient pressure (=130.68Å^3). The obtained value is $B = 126.8$ GPa and $B' = 17.1$.

Figures 3(a) and 3(b) display T dependence of the heat capacity C_{ac} and the phase shift obtained from the ac calorimetry measurements at selected pressures, respectively. All the data shown in Fig. 3 were taken on the heating process. Each $C_{ac}(T)$ curve shows a broad shoulder. In the data at 1.1 GPa, for example, the shoulder is seen at around $T = 27$ K, which is close to T_N at ambient pressure. Corresponding to the anomaly in C_{ac}, the phase shift exhibits a distinct dip. The phase shifts on the ac calorimetry, which means the phase differences of temperature oscillation between the heater and the specimen, are also sensitive to the presence of a phase transition.[13] Thus the anomalies in C_{ac} and the phase shift
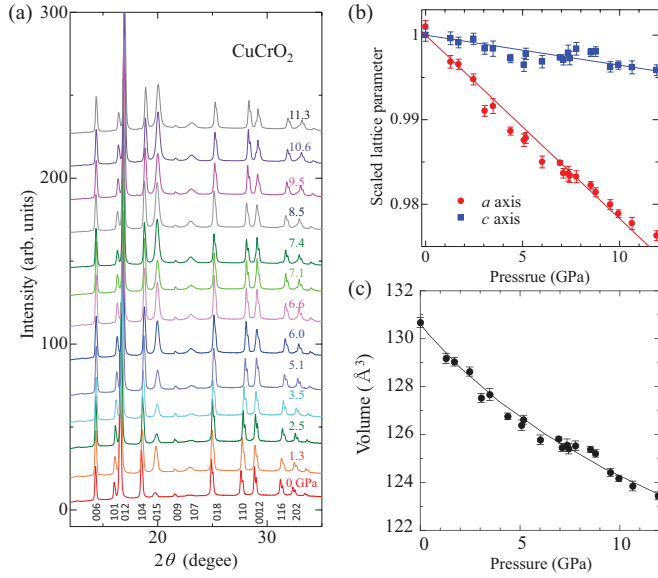
FIG. 2. (Color online) (a) Powder x-ray diffraction peak profiles of 2θ at room temperature under selected pressures. Numbers listed below the profiles denote *hkl* indices of the respective Bragg peaks. (b) Pressure dependencies of scaled lattice parameters in the hexagonal setting. Circles and squares represent the *a*- and *c*-axis lengths. The compressibility along the *a* and *c* axes is estimated by a linear fitting [solid lines shown in (b)]. (c) Unit-cell volume as a function of pressure. A solid line corresponds to Murnaghan's equation.

correspond to the magnetic (and ferroelectric) phase transition into the screw spiral magnetic order, and the temperature showing the anomaly in the phase is defined as T_N. (Broadened features of the anomalies in C_{ac} and the phase component are probably due to the presence of a slight pressure distribution in the sample chamber.) It is apparent that T_N is enhanced with increasing pressure. This result can be simply explained by the fact that the interlayer distance becomes shorter with increasing pressure. The shortening of the interlayer distance may stabilize a magnetically ordered state and then enhance T_N. In fact, such a relationship between the interlayer distance and T_N has been observed and discussed in the chemically substituted $ACrO_2$ family (A = alkali metal).[16]

Figure 4 shows T profiles of dielectric constant ε' along the [110] direction under various pressures. All the data are obtained at 100 kHz, though the data at 0 GPa are exceptionally taken in an ambient pressure condition without using the DAC. The respective data are scaled by their value at 60 K and vertically offset for clear comparison. The inset of Fig. 4 displays a magnified view of the data measured at 6.5, 8.6, and 10.2 GPa. At 0 GPa collected in the DAC, a remarkable peak structure is observed around the magnetic and ferroelectric transition temperature $T_N = 24$ K, which is consistent with a previous report.[2] With increasing pressure, the peak structure in ε' gradually shifts toward higher temperatures in accordance with the anomaly in C_{ac}. This result suggests that the spin-driven ferroelectric phase expands toward higher temperature by applying pressure. Meanwhile the amplitude of dielectric anomaly is gradually enhanced with increasing pressure up to about 4 GPa, shows a maximum at around 4 GPa, and then is suppressed with further increasing pressure. However,
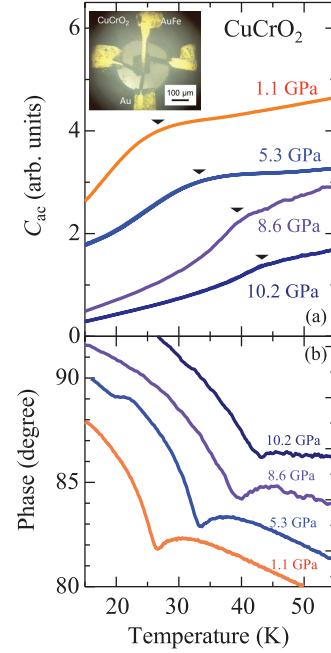

FIG. 3. (Color online) Temperature profiles of the heat capacity C_{ac} obtained by the ac calorimetry method and the phase component of C_{ac} under several pressures. Inset: Microscope image of CuCrO$_2$ with four lead wires in a pressure chamber.

the substantial dielectric anomaly remains up to the highest pressure studied here (10.2 GPa).

Figure 5 represents the electric field dependence of electric polarization along the [110] direction collected in various pressures at 5 K far below T_N. We measured electric polarization after cooling the specimen at $E = 5$ MV/m from a temperature above T_N. At ambient pressure collected in the DAC (0 GPa), a clear hysteresis loop can be seen. The coercive field E_c at 0 GPa is about 1×10^{-1} MV/m, which is much smaller than that of other spin-driven ferroelectrics. The smallness of E_c in CuCrO$_2$ has been discussed in terms of the smallness of the
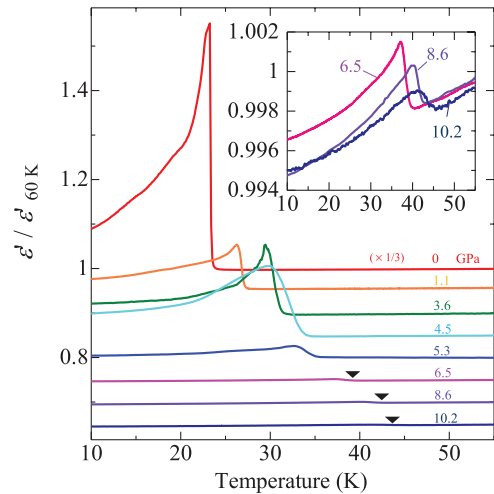

FIG. 4. (Color online) Temperature profiles of dielectric constant ε' scaled by the value at 60 K under several pressures. Black triangles indicate dielectric anomalies. Inset: A magnified view of the data at 6.5, 8.6, 10.2 GPa.
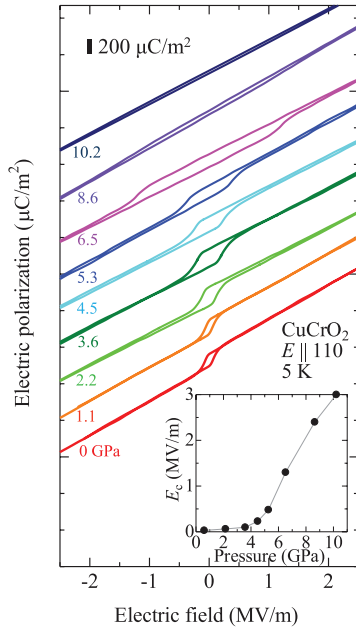
FIG. 5. (Color online) Ferroelectric hysteresis at various pressures at 5 K. Electric fields were applied parallel to the [110] direction in the hexagonal setting. The inset represents the coercive electric field (E_c) as a function of pressure. The gray line is a guide for the eyes.

in-plane magnetic anisotropy in the delafossite compound.[17] With increasing pressure, E_c increases monotonically. The pressure evolution of E_c is shown in the inset of Fig. 5. Up to 4 GPa at which the dielectric anomaly is the most enhanced, both E_c and the magnitude of spontaneous polarization increase gradually with increasing pressure. Above 4 GPa,
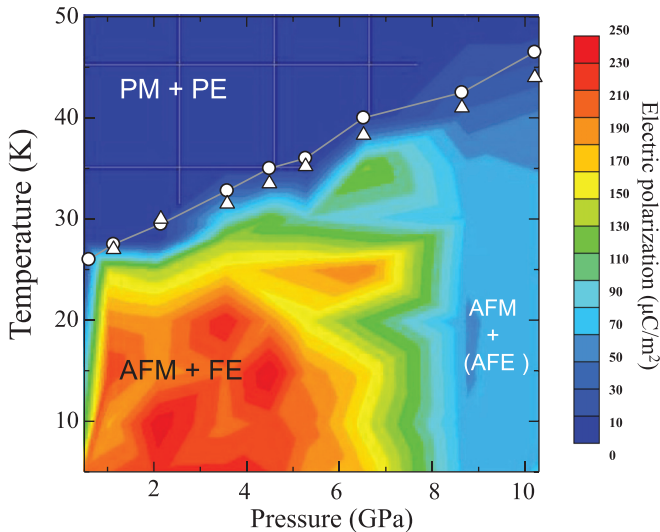

FIG. 6. (Color online) Pressure-temperature phase diagram with the contour plot of amplitude of spontaneous polarization along [110] (P_{110}). The contour plot of P_{110} is obtained from P-E hysteresis measurements at temperatures between 5 and 50 K by every 5-K step in several pressures. Each data of P_{110} is collected after electric field cooling. Here, PM, PE, AFM, FE, and AFE denote paramagnetic, paraelectric, antiferromagnetic, ferroelectric, and possible antiferroelectric phases, respectively.

E_c starts to increase divergently and reaches about 3 MV/m at 10.2 GPa. In contrast to the clear dielectric anomaly which remains up to 10.2 GPa (Fig. 4), spontaneous polarization as well as the hysteresis loop almost vanishes at 10.2 GPa. The rapid increase of E_c above 4 GPa is probably ascribed to the pressure-induced suppression of the spontaneous polarization above 4 GPa.

To summarize the obtained pressure effects on the magnetic and ferroelectric properties of CuCrO$_2$, we display in Fig. 6 the pressure-temperature phase diagram determined by the T profiles of C_{ac} (open triangle symbols) and ε' (open circle symbols). The contour plot of spontaneous polarization along [110] direction obtained from the P-E hysteresis measurements is also shown in the phase diagram of Fig. 6. As one can see, the amplitude of the spontaneous polarization below T_N increases at low pressure, shows a maximum at around $2 \sim 4$ GPa, and then monotonically decreases above about 5 GPa. Eventually, it almost vanishes above around 8 GPa. The pressure evolution of the spontaneous polarization is similar to that of the amplitude of the dielectric anomaly (see Fig. 4).

IV. DISCUSSION

To explain the above-mentioned pressure effect on the spin-driven ferroelectricity in CuCrO$_2$, i.e., the suppression of the spontaneous polarization and the enhancement of the coercive field by applying pressure, we propose two possible scenarios. The first scenario is ascribed to a pressure-induced ferroelectric-antiferroelectric transition accompanied by a magnetic transition due to variations of intra- and interlayer magnetic couplings by applying pressure. As mentioned in Ref. 16, the Cr-layer spacing and the interlayer magnetic integral J' play an important role in determining T_N in the ACrO$_2$ family. In CuCrO$_2$, T_N (≈ 45 K) at 10.2 GPa is almost comparable to that of nonpressurized, ordered rocksalt NaCrO$_2$ (≈ 39 K) and LiCrO$_2$ (≈ 59 K), in which their ground state is expected to be spin-driven antiferroelectric due to alternate stacking of the spin chirality.[1] In ordered rocksalt LiCrO$_2$ in which the O-Li-O bond path tilts from the c axis, the interlayer Cr-Cr distance is $\sim 10\%$ shorter than that of delafossite CuCrO$_2$ with the straight O-Cu-O bond path parallel to the c axis. According to the result of XRD under high pressure, however, the pressure variation of the c axis is only about 1%, and there are no indications of any structural phase transition. Thus the observed abrupt suppression of the spontaneous polarization in pressurized CuCrO$_2$ could be induced by the change in the interlayer magnetic interaction through the slight change in the c-axis length.

Furthermore, as shown in Fig. 1, the amplitude of the dielectric anomaly at T_N in LiCrO$_2$ is much smaller than that in CuCrO$_2$. This behavior can be explained by a qualitative, phenomenological analysis of the antiferroelectric transition. In general, the dielectric constant will not be particularly large at the antiferroelectric Curie temperature, whether the transition nature is first or second order, which is contrary to the ferroelectric one.[18] As seen in Figs. 4 and 5, the amplitudes of the dielectric anomaly and the spontaneous polarization are suppressed in pressurized CuCrO$_2$. This could indicate that the application of pressure on CuCrO$_2$ gives rise to a ferroelectric-antiferroelectric transition accompanied by a

magnetic transition through variations of intra- and interlayer magnetic coupling.

The other scenario is related to the structural domain rearrangement induced by the uniaxial pressure. First, let us consider the structural and magnetic domains in $CuCrO_2$. There is threefold rotation axis along the c axis above T_N. Below T_N, the threefold rotation symmetry is broken by a lattice distortion accompanied by the screw spiral spin order and resultant ferroelectricity, and then three structural $120°$ domains are formed.[19] In addition to the structural domains, there is the spin-chirality degree of freedom corresponding to the handedness on the spiral spin ordered phase. Eventually, there are six structural-magnetic domains, i.e., $60°$ domain structures. According to a previous report about the domain arrangement determined by measurements of strain and XRD,[19] the sample length along the [110] direction parallel to P shrinks below T_N. If there is a uniaxial component in the external pressure, these domains can be arranged along the uniaxial direction due to the anisotropic distortion mentioned above. Such arrangement makes E_c larger, as described in Ref. 17. In the case of the DAC using glycerin as the pressure-transmitting medium, the uniaxial component in the external pressure may be generated along the pressurizing axis (i.e., the [110] direction in this situation) by the solidification of the glycerin above about 6 GPa at 300 K.[20] As the ruby fluorescence line broadens, however, other than a gradual broadening (not shown), no sudden anomaly has been observed around 6 GPa. The domain arrangement by uniaxial pressure in another multiferroics delaffosite $Cu(Fe,Ga)O_2$ has been reported in Ref. 21. According to the report, extremely small uniaxial ($\sim$30 MPa) pressure can have an influence on the rearrangement of the structural domains. This scenario can explain only the enhancement of E_c by applying pressure, but not the suppression of the spontaneous polarization. Thus we speculate that the observed pressure effects are ascribed to the combination of the above-mentioned two scenarios.

V. SUMMARY

In summary, we have successfully established a measurement system which allows dielectric, ferroelectric, and ac calorimetric measurements under high-pressure conditions by using a diamond anvil cell. Using the system, we investigated pressure effects on the structure and magnetoelectric properties of a multiferroic triangular-lattice antiferromagnet, $CuCrO_2$. It was found that the magnetic transition temperature into the spin-spiral ferroelectric ordered phase T_N remarkably increases with pressurization. However, the magnitude of the dielectric anomaly at T_N is suppressed by applying pressure, and the magnitude of the spontaneous polarization below T_N is abruptly suppressed at around 8 GPa. These results suggest that a ferroelectric-antiferroelectric transition has occurred as the Cr-layer spacing becomes shorter and the interlayer exchange integral becomes larger with pressurization. Furthermore, the coercive field for the polarization reversal becomes large with pressurization, which can be interpreted in terms of the magnetoelectric domain rearrangement. The present results clearly demonstrate that the application of pressure can be an effective perturbation in the investigation and tuning of magnetoelectric properties in multiferroic materials.

[1] S. Seki, Y. Onose, and Y. Tokura, Phys. Rev. Lett. **101**, 067204 (2008).

[2] K. Kimura, H. Nakamura, K. Ohgushi, and T. Kimura, Phys. Rev. B **78**, 140401(R) (2008).

[3] H. Kadowaki, H. Kikuchi, and Y. Ajiro, J. Phys.: Condens. Matter **2**, 4485 (1990).

[4] M. Poienar, F. Damay, C. Martin, V. Hardy, A. Maignan, and G. Andre, Phys. Rev. B **79**, 014412 (2009).

[5] M. Soda, K. Kimura, T. Kimura, M. Matsuura, and K. Hirota, J. Phys. Soc. Jpn. **78**, 124703 (2009).

[6] T. Arima, J. Phys. Soc. Jpn. **76**, 073702 (2007).

[7] J. L. Soubeyroux, D. Fruchart, J. C. Marmeggi, W. J. Fitzgerald, C. Delmas, and G. Le Flem, Phys. Status Solidi A **67**, 633 (1981).

[8] T. Otani, Masters thesis, Osaka University, 2011.

[9] H. Kadowaki, H. Takei, and K. Motoya, J. Phys.: Condens. Matter **7**, 6879 (1995).

[10] T. Ishidate, S. Abe, H. Takahashi, and N. Môri, Phys. Rev. Lett. **78**, 2397 (1997).

[11] T. Aoyama, A. Miyake, K. Shimizu, and T. Kimura, J. Phys. Soc. Jpn. **81**, Supplement B SB036 (2012).

[12] Y. Seto, D. Nishio-Hamane, T. Nagai, and N. Sata, Rev. High Pressure Sci. Technol. **20**, 269 (2010).

[13] A. Eichler and W. Gey, Rev. Sci. Instrum. **50**, 1445 (1979).

[14] T. Zhao, M. Hasegawa, H. Takei, T. Kondo, and T. Yagi, Jpn. J. Appl. Phys., Part 1 **35**, 3535 (1996).

[15] J. Pellicer-Porres, A. Segura, Ch. Ferrer-Roca, D. Martínez-García, J. A. Sans, E. Martínez, J. P. Itié, A. Polian, F. Baudelet, A. Muñoz, P. Rodríguez-Hernández, and P. Munsch, Phys. Rev. B **69**, 024109 (2004).

[16] S. Angelov and J. P. Doumerc, Solid State Commun. **77**, 213 (1991).

[17] K. Kimura, H. Nakamura, S. Kimura, M. Hagiwara, and T. Kimura, Phys. Rev. Lett. **103**, 107201 (2009).

[18] C. Kittel, Phys. Rev. **82**, 729 (1951).

[19] K. Kimura, T. Otani, H. Nakamura, Y. Wakabayashi, and T. Kimura, J. Phys. Soc. Jpn. **78**, 11 (2009).

[20] N. Tateiwa and Y. Haga, Rev. Sci. Instrum. **80**, 123901 (2009).

[21] T. Nakajima, S. Mitsuda, T. Nakamura, H. Ishii, T. Haku, Y. Honma, M. Kosaka, N. Aso, and Y. Uwatoko, Phys. Rev. B **83**, 220101 (2011).